ELSEVIER

International Journal of Heat and Fluid Flow 21 (2000) 146–155

International Journal of HEAT AND FLUID FLOW

www.elsevier.com/locate/ijhff

Film-cooling holes with expanded exits: near-hole heat transfer coefficients

Michael Gritsch *, Achmed Schulz, Sigmar Wittig

Lehrstuhl und Institut für Thermische Strömungsmaschinen, Universität Karlsruhe (T.H.), Kaiserstrasse 12, 76128 Karlsruhe, Germany

Received 26 April 1999; accepted 27 September 1999

Abstract

This paper presents detailed measurements of local heat transfer coefficients in the vicinity of three film-cooling holes with different hole geometries including a standard cylindrical hole and two holes with a diffuser shaped exit portion (i.e. a fanshaped and a laidback fanshaped hole). Tests were conducted over a range of blowing ratios $M = 0.25 \ldots 1.75$ at an external crossflow Mach number of 0.6 and a coolant-to-mainflow density ratio of 1.85. Additionally, the effect of the internal coolant supply Mach number was addressed. Surface temperatures downstream of the injection location were measured by means of an infrared camera system and used as boundary conditions for a finite element analysis to determine surface heat fluxes and heat transfer coefficients downstream of the injection location. Furthermore, the superposition method was applied to evaluate the overall film-cooling performance of the hole geometries investigated by combining heat transfer and adiabatic cooling effectiveness data. As compared to the cylindrical hole, both expanded holes show significantly lower heat transfer coefficients downstream of the injection location, particularly at high blowing ratios. The laidback fanshaped hole provides a better lateral spreading of the injected coolant than the fanshaped hole which leads to lower laterally averaged heat transfer coefficients. Coolant passage crossflow Mach numbers affect the flowfield of the jet being ejected from the hole and, therefore, have an important impact on film-cooling performance.

Keywords: Film cooling; Heat transfer coefficients; Fanshaped holes

Notation

D	film-cooling hole diameter
DR	coolant-to-mainflow density ratio
h	local heat transfer coefficient
h_f	local heat transfer coefficient at $\Theta = 0$, Eq. (1)
I	coolant-to-mainflow momentum flux ratio
L	film-cooling hole length measured along the hole centerline
M	blowing ratio
Ma	Mach number
NHFR	net heat flux reduction, Eq. (3)
$\dot{q}''$	surface heat flux
Re_D	Reynolds number based on film-cooling hole diameter
T_t	total temperature
T_{rec}	recovery temperature
Tu	turbulence intensity
x	streamwise distance from downstream edge of the film-cooling hole
z	lateral distance from centerline of the film-cooling hole

Greeks

α	angle of hole inclination
δ_{99}	boundary layer thickness, 99% point
η	local film-cooling effectiveness, Eq. (2)
Θ	dimensionless temperature ratio, Eq. (4)

Subscripts

0	no injection case
c	coolant conditions
m	mainflow conditions
AW	adiabatic wall conditions ($\dot{q}'' = 0$)
W	diabatic wall conditions ($\dot{q}'' \neq 0$)

Superscripts

$-$	laterally averaged value
$=$	spatially averaged value

1. Introduction

Improving the performance of gas turbines can be achieved by increasing the turbine inlet temperature. This requires highly effective cooling techniques to maintain the temperature of the components in contact with the hot gases at acceptable

* Corresponding author. Present address: ABB Alstom Power Technology Ltd, Department of Thermo- and Aerodynamics, 5405 Baden-Dättwil, Switzerland.

E-mail address: michael.gritsch@ch.abb.com (M. Gritsch).

0142-727X/00/$ - see front matter
PII: S0142-727X(99)00076-4

levels. Film-cooling is widely used to protect gas turbine blades from hot gases by injecting compressor bleed air through discrete holes in the blade surface.

The heat transfer to a film-cooled blade (Goldstein, 1971) can be defined as

$$\dot{q}'' = h_f(T_{AW} - T_W). \tag{1}$$

Usually, the adiabatic wall temperature T_{AW} is presented non-dimensionalized as the adiabatic film-cooling effectiveness

$$\eta = \frac{T_{AW} - T_{t,m}}{T_{t,c} - T_{t,m}}. \tag{2}$$

Sen et al. (1996) introduced the net heat flux reduction (NHFR) which quantifies the reduction of the heat transfer to the blade with film-cooling as compared to without film-cooling

$$\begin{aligned} \mathrm{NHFR} &= 1 - \frac{\dot{q}''}{\dot{q}_0''}, \\ &= 1 - \frac{h_f(T_{AW} - T_W)}{h_0(T_{t,m} - T_W)}. \end{aligned} \tag{3}$$

Using a dimensionless temperature

$$\Theta = \frac{T_{t,m} - T_{t,c}}{T_{t,m} - T_W}, \tag{4}$$

Eq. (3) can be written as

$$\mathrm{NHFR} = 1 - \frac{h_f}{h_0}(1 - \eta\Theta). \tag{5}$$

Protecting the blade surface by means of film-cooling is established by reducing the adiabatic wall temperature and reducing the heat transfer to the surface. It becomes evident that NHFR combines and quantifies both effects of film-cooling. Both the film-cooling effectiveness as well as the local heat transfer coefficient have to be known to assess the overall performance of film-cooling.

Most of the research in the field of film-cooling during the last decades dealt with the determination of the film-cooling effectiveness η, while the heat transfer coefficient h_f has received less attention. It was assumed that the convective heat transfer coefficient remains unchanged by the coolant injection ($h_f = h_0$). However, this is only valid far downstream of the injection location. In the vicinity of the hole the drastically altered flow-field has a strong impact and can result in a substantial reduction or augmentation of the heat transfer. Therefore, the determination of the heat transfer coefficient h_f with film-cooling is essential for predicting the overall thermal load on the blade.

For the case of streamwise injection through discrete cylindrical holes, most studies stated that h_f/h_0 is unity except in the vicinity of the hole where increased values were found. Hay et al. (1985) reported that h_f/h_0 increases with blowing ratio. For a streamwise injection at an inclination angle of 35° the maximum value was found to be 1.35. Heat transfer coefficients up to 60% higher as without injection were reported by Liess (1975) for near-hole locations at elevated blowing ratios. At low blowing ratios, however, heat transfer coefficients with injection can be lower than without injection due to the fact that the injected mass thickens the boundary layer (Eriksen and Goldstein, 1974).

Sen et al. (1996) and Schmidt et al. (1996) found that compound angle injection results in higher film-cooling effectiveness as compared to streamwise injection at a given momentum ratio. However, the heat transfer rates are substantially enhanced due to an increased jet–crossflow interaction. Therefore, the overall performance, combining the effects of reducing blade temperature and heat transfer, was lower for compound angle holes. These findings have been confirmed by studies of Ekkad et al. (1997a,b) and Cho and Goldstein (1995).

The geometry of the film-cooling holes has received recent attention in attempts to optimize the cooling process. Holes with expanded exits have been shown to be superior to standard cylindrical holes. Goldstein et al. (1974) reported significantly increased film-cooling effectiveness in the vicinity of the hole as well as an improved lateral spreading of the ejected jet for laterally expanded cooling holes. In a study investigating aerodynamic losses on a transonic linear cascade, Haller and Camus (1983) showed that laterally expanded cooling holes offer higher film-cooling effectiveness without any additional loss penalty. Maki and Jakubowski (1986) experimentally studied the benefits of trapezoidal shaped holes as compared to standard cylindrical holes. They reported the heat transfer coefficient of the shaped holes to be up to 20% lower in the vicinity of the hole ($x/D < 50$), particularly at low and medium blowing ratios.

Numerical studies investigating the effect of hole geometry on film-cooling performance revealed that flow inside shaped cooling holes is highly complex (Giebert et al., 1997) and very sensitive to how the coolant is supplied to the hole (Kohli and Thole, 1997). Hay et al. (1983) documented the effect of internal crossflow on the discharge coefficient of film-cooling holes while Burd and Simon (1997) experimentally studied the effect of coolant feed direction on hole exit flow and adiabatic effectiveness.

Hyams and Leylek (1997) stated that heat transfer coefficients for a hole with a laterally diffused exit, a hole with a forward diffused exit, and a standard cylindrical hole at $M = 1.25$ and $\mathrm{DR} = 1.6$ are slightly elevated as compared to an undisturbed boundary layer. For the laterally expanded hole the highest heat transfer coefficients were found ($h_f/h_0 = 1.3$ at $x/D = 2$), while the heat transfer coefficients for the cylindrical reference hole and the forward expanded hole were about the same.

In a previous paper by Gritsch et al. (1998) film-cooling effectiveness distributions of a standard cylindrical, a laterally expanded as well as a laterally forward expanded film-cooling hole were presented. Both expanded holes showed profoundly improved thermal protection as compared to the cylindrical hole. The laidback fanshaped hole, however, provides a better lateral spreading of the film ejected from the hole than the fanshaped hole which leads to higher laterally averaged film-cooling effectiveness. Flow-field measurements performed by Thole et al. (1998) revealed that for both expanded holes jet penetration as well as velocity gradients in the mixing region were drastically reduced.

This paper presents the heat transfer coefficient results of a comprehensive film-cooling study conducted at the Institut für Thermische Strömungsmaschinen (ITS), University of Karlsruhe. Two-dimensional distributions of the heat transfer coefficient in the near-field of a single, scaled-up film-cooling hole with and without exit expansions are measured by means of an infrared camera system. The main parameters of the flow, such as Mach numbers in the main channel as well as in the coolant supply passage, density ratio, boundary layer thickness, and blowing ratios can be assumed to be representative for typical gas turbine applications.

2. Experimental apparatus

The present investigation was carried out in a continuous flow wind tunnel. The air supply was provided by a high pressure, high temperature (HPHT) test facility. The

Table 1
Operating conditions of the film-cooling test rig

Coolant temperature	$T_{t,c}$	290 K
Blowing ratio	M	0.25 ... 1.75
Temperature ratio	$T_{t,c}/T_{t,m}$	0.54
Internal Mach number	Ma_c	0, 0.3, 0.6
External Mach number	Ma_m	0.6
Internal Reynolds number	$Re_{D,c}$	up to 2.5×10^5
External Reynolds number	$Re_{D,m}$	0.75×10^5
External BL thickness	δ_{99}/D	0.5
External turbulence intensity	Tu_m	<2%
Internal turbulence intensity	Tu_c	1%

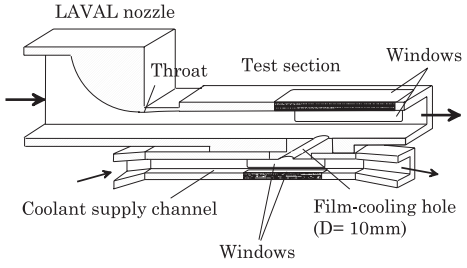

Fig. 1. Film-cooling test section.

coolant-to-mainflow temperature ratio was kept at 0.54 (DR = 1.85) for all test cases. The operating conditions are shown in Table 1. Further details of the test rig design, the flow conditions, and on preliminary testing were given by Wittig et al. (1996).

The film-cooling test rig consists of a primary loop representing the external flow and a secondary loop representing the internal flow (see Fig. 1).

2.1. Primary loop

The air supplied by the HPHT test facility passes a metering orifice and flow straighteners before entering the test section through a laval nozzle. Flow Mach numbers up to 1.2 can be established. The test section is 90 mm in width and 41 mm in height. The top wall opposite to the film-cooling hole exit is furnished with a sapphire window required for surface temperature measurements using an infrared camera system.

2.2. Secondary loop

Flow for the secondary loop is provided by the HPHT test facility, too. However, the total pressure in the secondary loop can be set independently from the primary loop. The flow in the secondary loop is driven by an additional blower. Thus, the Mach number (up to 0.6) can be set by adjusting the volume flow rate circulating in the secondary loop. The cross-sectional area at the film-cooling hole is 60 mm in width and 20 mm in height. Due to a 'closed loop' design of the secondary loop, the flow rate through the film-cooling hole is obtained directly, independently of the crossflow rate. This results in very accurate measurements of the flow rate through the film-cooling hole (Wittig et al., 1996).

2.3. Film-cooling hole geometries

All tests are carried out using single, scaled-up film-cooling holes with an inclination angle of $\alpha = 30°$ injecting in streamwise direction. The holes are sharp edged and the interior surfaces are aerodynamically smooth. In total, three hole geometries (a cylindrical hole and two holes with an expanded exit portion) are tested (see Fig. 2). The diameter of the cylindrical hole and the diameter of the cylindrical inlet section of the expanded holes is 10 mm. The length-to-diameter ratio L/D is 6 for all hole geometries. The lateral expansion angle of both expanded holes is 14°, resulting in a hole width of 30 mm at the hole exit. The forward expansion angle of the laidback fanshaped hole is 15°, resulting in a hole length of 40 mm at the hole exit. The exit-to-entry area ratio of the fanshaped and laidback fanshaped hole is 3.0 and 3.1, respectively (areas perpendicular to hole axis).

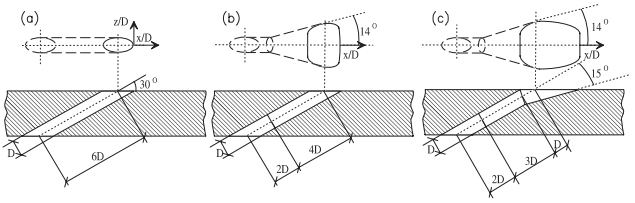

Fig. 2. Cylindrical, fanshaped, and laidback fanshaped film-cooling hole geometries.

The hole geometries were decided in cooperation with the industrial partners involved in the present research program. The chosen geometry of the expanded holes is in agreement with the suggestion of Hay and Lampard (1995) that the length of the cylindrical section at the hole entry of the expanded holes should be at least two hole diameters. This is to allow the flow to reattach before entering the expanded section and, therefore, to improve the diffusion of the flow. A larger expansion angle would lead to an improved lateral coverage of the ejected film but flow separation in the diffuser section of the hole could occur. Therefore, the chosen expansion angle must be seen as a compromise.

For the fanshaped and the laidback fanshaped hole, the calculation of the blowing ratio is based on the inlet cross-sectional area of these holes. Thus, the blowing ratio of the shaped holes can be directly compared to those of the cylindrical hole. Same blowing ratio is synonymous with same amount of coolant ejected provided that the mainflow conditions remain unchanged. This makes it more convenient to evaluate the effect of contouring the hole.

3. Measurement technique

The superposition approach to film-cooling is an accepted method of dealing with problems of varying wall temperatures and was first described by Metzger and Fletcher (1971) and Choe et al. (1974). It arises from the linearity and homogeneity of the simplified boundary layer differential equations. In this case, the heat transfer is usually defined as

$$\dot{q}'' = h(T_{t,m} - T_W). \tag{6}$$

Eckert (1984) showed that this approach is equivalent to Goldstein's approach (Eq. (1)). They can be combined to

$$\frac{h}{h_0} = \frac{h_f}{h_0}(1 - \eta\Theta). \tag{7}$$

The findings of Metzger and Fletcher (1971) who showed the linearity of h with Θ were extended by Forth et al. (1985) to compressible, variable properties flow situations. When plotting h/h_0 versus Θ, the axes intercepts are h_f/h_0 at $\Theta = 0$ and

$1/\eta$ at $h/h_0 = 0$. To determine h_f and η, at least two data sets at two different Θ are required.

Several techniques for determining the local heat transfer coefficient have been applied in the past. Transient measuring techniques like liquid crystals (Shen et al., 1991) or thin film heat flux gauges (Teekaram et al., 1989) were used in a short duration blow-down wind tunnel. Results from mass transfer experiments such as swollen polymer surface in conjunction with laser holographic interferometry (Goldstein and Taylor, 1982; Hay et al., 1993) as well as naphtalene sublimation (Cho and Goldstein, 1995; Häring et al., 1995) were believed to be transferable to heat transfer problems using the heat/mass transfer analogy. Eriksen and Goldstein (1974), Ligrani et al. (1991) and Sen et al. (1996) used electrical heater foils to apply a wall heat flux in steady-state experiments. This technique has also been used at ITS before (Scherer et al., 1991; Martiny et al., 1997). The major drawback of the heater foils is that they cannot be used at elevated temperatures. Thus, experiments using heater foils were performed at coolant-to-mainflow density ratios close to unity. For the determination of the heat transfer coefficient, however, it is important to perform the heat transfer experiments at the same flow conditions as the adiabatic wall experiments. This can be achieved by keeping the coolant-to-mainflow temperature ratio unchanged and varying Θ only by varying the wall temperature. Therefore, another technique of determining the local heat transfer coefficient has been applied in the present investigation (Gritsch et al., 1999).

The test plate used for acquiring heat transfer coefficients consists of a copper block which is maintained at a constant temperature by internal water cooling (Fig. 3). The copper block is topped with a 3 mm layer of a high temperature plastic called (TECAPEK) with a thermal conductivity of 0.21 W/mK and a maximum operating temperature of about 570 K to reduce heat conduction in streamwise and lateral direction. Surface temperatures are measured by means of an AGEMA Thermovision 870 IR camera system.

The IR camera system provides a two-dimensional distribution of the temperature on the plate surface. The image of the test plate surface is digitized into an array of 140×140 pixels. Accounting for the optical setup used with the IR camera a spatial resolution 0.8×0.8 mm^2 per pixel can be achieved. The test plate surface is covered by black paint of a known emissivity of 0.95. Seven thermocouples distributed on the plate surface are used for an in situ calibration of the IR camera system to increase the accuracy of the temperature measurements. Details of the in situ calibration procedure are given by Martiny et al. (1996).

A finite element analysis is performed to calculate the three-dimensional temperature distribution in the test plate and to derive the heat flux $\dot{q}''$ perpendicular to the surface of the test plate. The surface temperature of the test plate and the temperature of the water circulating through the copper block are used as boundary conditions for the finite element analysis. Additional thermocouples located in the contact zone of plastic and copper were used to validate the appropriate modelling of the test plate. Using Eq. (6), the heat transfer coefficient h is calculated from the surface heat flux and free-stream-to-wall temperature difference. Note that the mainflow total temperature $T_{t,m}$ in Eqs. (2)–(4) and (6) has to be replaced by the recovery temperature $T_{rec,m}$ for compressible flows as investigated in the present study ($Ma_m = 0.6$).

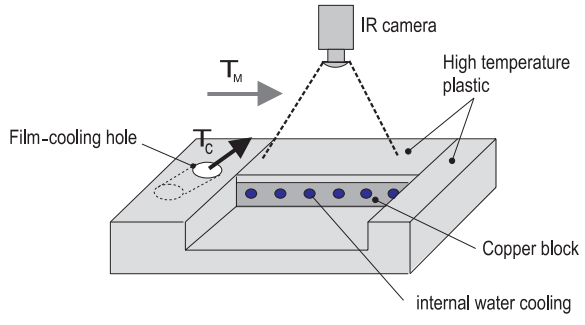

Fig. 3. Heat transfer test plate.

Finally, the heat transfer coefficient h_f is determined from a linear extrapolation according to Eq. (7). To perform this extrapolation a second set of data at the same flow conditions but a different Θ is needed. It is obvious to use the wall temperature distribution for the adiabatic case presented in a previous paper (Gritsch et al., 1998) as the second data set. The calculation procedure has to be performed for each pixel of the IR camera image to receive a two-dimensional distribution of the heat transfer coefficient h_f.

4. Results and discussion

The results of the present investigation will be presented in terms of two-dimensional heat transfer coefficient distributions, as well as of laterally and spatially averaged heat transfer coefficients. Local heat transfer coefficients h_f will always be normalized using the heat transfer coefficients h_0 of the no blowing case at the same location. Note that h_0 was determined from preliminary tests with the film-cooling holes blocked which were performed to validate the data reduction scheme for the determination of the local heat transfer coefficients. The results showed good agreement to heat transfer coefficients calculated from correlations for turbulent boundary layer heat transfer provided by Kays and Crawford (1980).

Since changes in heat transfer due to coolant injection are expected to be most distinct close to the hole the results presented will focus on the heat transfer coefficients in the vicinity of the hole ($x/D < 8$). As a baseline case, a mainflow Mach number of $Ma_m = 0.6$ and a coolant supply passage Mach number of $Ma_c = 0.0$ (i.e. plenum condition) have been chosen from the test matrix. For this flow configuration the effect of hole geometry and blowing ratio on local as well as laterally and spatially averaged heat transfer coefficient will be discussed. Further on, the effect of the coolant supply passage Mach number on the heat transfer coefficient distribution will be presented for all hole geometries and compared to the baseline case. Additionally, the present heat transfer results will be combined with previous film-cooling effectiveness results to evaluate the overall film-cooling performance of the holes investigated.

The main contribution to uncertainty in calculating the heat transfer coefficient h_f is the fact that two data sets at identical flow conditions (M, Ma_m, and T_c/T_m) are needed to determine h_f from a linear extrapolation. Particularly for the cylindrical hole, the jet position relative to the wall is very sensitive to slight variations of the blowing ratio at high blowing ratios. The uncertainty in setting the external and internal Mach number as well as the blowing ratio is within 3% and in setting the temperature ratio is 1.5%. The maximum deviation of the temperatures measured by means of the IR camera system from the temperatures of the surface thermocouples are less than 1.5 K (Martiny et al., 1996). Combining these uncertainties (Kline and McClintock, 1953) results in an average uncertainty of 4% for the local and laterally averaged heat transfer coefficient. The maximum uncertainty is calculated to be 9%.

4.1. Local heat transfer distributions

Fig. 4 presents the local heat transfer coefficient ratios h_f/h_0 in the near-field of the cylindrical, the fanshaped, and the laidback fanshaped hole at three different blowing ratios ($M = 0.5, 1.0$, and 1.5). For the cylindrical hole, heat transfer coefficient ratios are very low in the centerline region at the lowest blowing ratio. This is due to the fact that the velocity of the injected jet is much lower than of the freestream which reduces the heat transfer as compared to the no blowing case. Additionally, the injected mass thickens the boundary layer. At higher blowing ratios the injected jet has separated from the surface. The enhanced jet–mainflow interaction leads to elevated heat transfer coefficients off-centerline, particularly at $z/D = 0.5$.

For the fanshaped hole, a profound decrease of the heat transfer coefficient level is found at elevated blowing ratios as compared to the cylindrical hole. The increased cross-sectional area at the exit of these holes decreases the exit momentum flux of the jet and, therefore, reduces the penetration of the jet into the mainflow as compared to standard cylindrical holes, which becomes obvious particularly at high blowing ratios. The injected coolant leads to lower near-wall velocities and thickens the boundary layer as reported by Thole et al. (1998) who performed flowfield measurements using the same hole geometry as in the present study. Both effects reduce the heat transfer level. Low heat transfer coefficients are found for all blowing ratios considered.

The heat transfer coefficients downstream of the laidback fanshaped hole are found to be similar to the fanshaped hole. The spreading of the low heat transfer region extends further in z-direction as compared to the fanshaped hole. This agrees with the results of the film-cooling effectiveness measurements of Gritsch et al. (1998) where an increased spreading of the jet exiting the laidback fanshaped hole was reported. Contrary to the fanshaped hole, minimum heat transfer coefficients are found off-centerline at $z/D = 1.5$ due to the spreading of the coolant in the laidback portion of the hole.

4.2. Laterally averaged heat transfer coefficients

To account for the lateral spreading of the jet local heat transfer coefficients are averaged across the lateral span ($z/D = \pm 2.75$) which corresponds to the approximate maximum extent to which film coverage was observed resulting in a laterally averaged heat transfer coefficient

$$\overline{\frac{h_f}{h_0}}(x/D) = \frac{1}{5.5}\int_{z/D=-2.75}^{z/D=2.75} \frac{h_f}{h_0}(x/d, z/D)\,\mathrm{d}(z/D). \tag{8}$$

To check the capability of the present measuring technique laterally averaged heat transfer coefficients for the cylindrical hole are compared to previously published data. To be consistent with previous studies the local heat transfer coefficient for this case is averaged for $z/D = \pm 1.5$ to simulate a nominal $s/D = 3$, which was used in most of the published studies (see Table 2).

It is well known that the density ratio and the blowing ratio are independent parameters for film-cooling flows. Only if both are matched, the flow field in the vicinity of the hole remains unchanged and a direct comparison with literature data is possible. Major problems, however, arose from the fact that most of the past studies looked at isothermal jet injection (DR = 1.0) while a more realistic density ratio DR = 1.85 is used in the present study. This made it difficult to compare the present data to those from the literature. However, as can be seen from Fig. 5, the heat transfer coefficients of the present study cover the same range as those taken from the literature while certain discrepancies occur immediately downstream of the injection location which might be attributed to the altered flow field due to the differences in density ratios.

The laterally averaged heat transfer coefficient distributions for the three holes studied are shown in Fig. 6. For the cylindrical hole, two different regimes can be detected. At low blowing ratios, $\overline{h_f/h_0}$ increases monotonically as x/D increases while at high blowing ratios $\overline{h_f/h_0}$ decreases monotonically. As one would expect, $\overline{h_f/h_0}$ tends towards unity for high x/D. For both shaped holes, $\overline{h_f/h_0}$ increases monotonically as x/D increases. Near the injection location $\overline{h_f/h_0}$ is very low. For all hole geometries considered, the streamwise distance at which the heat transfer coefficient becomes affected by cooling injection exceeds 8 hole diameters downstream of the injection location.

Fig. 7 presents the laterally averaged heat transfer coefficient plotted versus blowing ratio at $x/D = 3$ and 7. For the cylindrical hole, $\overline{h_f/h_0}$ increases monotonically with M. At high blowing ratios, $\overline{h_f/h_0}$ is profoundly increased as compared to both shaped holes. Minimum heat transfer coefficients for both shaped holes are found at medium blowing ratios. For all blowing ratios, however, $\overline{h_f/h_0}$ for the laidback fanshaped hole is up to about 20% lower than for the fanshaped hole. The results for the shaped holes are consistent with the data reported from Maki and Jakubowski (1986) for trapezoidal holes at DR = 1.6 and $x/D = 11$ which are added to the plot. Their results confirm that the heat transfer coefficients of shaped holes level are much lower as compared to the cylindrical hole. Minimum heat transfer coefficients were reported at medium blowing ratios of about $M = 1$.

4.3. Effect of coolant supply crossflow Mach number

Thus far, none of the film-cooling heat transfer studies reported have investigated the effect of a crossflow at the hole entry. A plenum, widely used to feed the film-cooling holes, is not necessarily a correct means to represent the internal coolant supply passage of an airfoil. To evaluate the effect of coolant supply passage crossflow three representative crossflow conditions have been chosen from the test matrix. These comprise coolant passage Mach numbers $Ma_c = 0.0$ (i.e. plenum condition), 0.3, and 0.6 at a nominal blowing ratio of $M = 1.0$. Results are presented in Fig. 8.

For the cylindrical hole, coolant supply crossflow has only a rather small effect on the laterally averaged heat transfer coefficient (about 10%), while for the shaped holes an increase of up to 15% (fanshaped) and 30% (laidback fanshaped) in $\overline{h_f/h_0}$ is found when the coolant supply crossflow Mach number is raised from $Ma_c = 0.0$ to 0.6. Gritsch et al. (1998) reported an increase of the laterally averaged film-cooling effectiveness of up to 30% for the cylindrical and 15–20% for the shaped holes at $M = 1.0$ when Ma_c is raised from 0.0 to 0.6.

For the cylindrical hole, flowfield measurements performed by Thole et al. (1997) showed that the ejected jet stays closer to the surface at elevated coolant supply Mach numbers which results in increased film-cooling effectiveness. For the heat transfer coefficients, the turbulence intensity inside the ejected jet, which is strongly affected by the coolant supply Mach number, becomes an important issue, particularly for the shaped holes, where the jet covers nearly the whole span (see Fig. 4). Elevated turbulence intensities are found at increased coolant supply Mach numbers leading to increased heat transfer inside the jet and, since the jet covers nearly the whole span, to increased laterally averaged heat transfer coefficients. The jet ejected through the cylindrical hole, however, covers only a small part of the span. Thus, the laterally averaged heat tranfer coefficient is dominated by the heat transfer coefficients outside the jet which are only slightly affected by the coolant

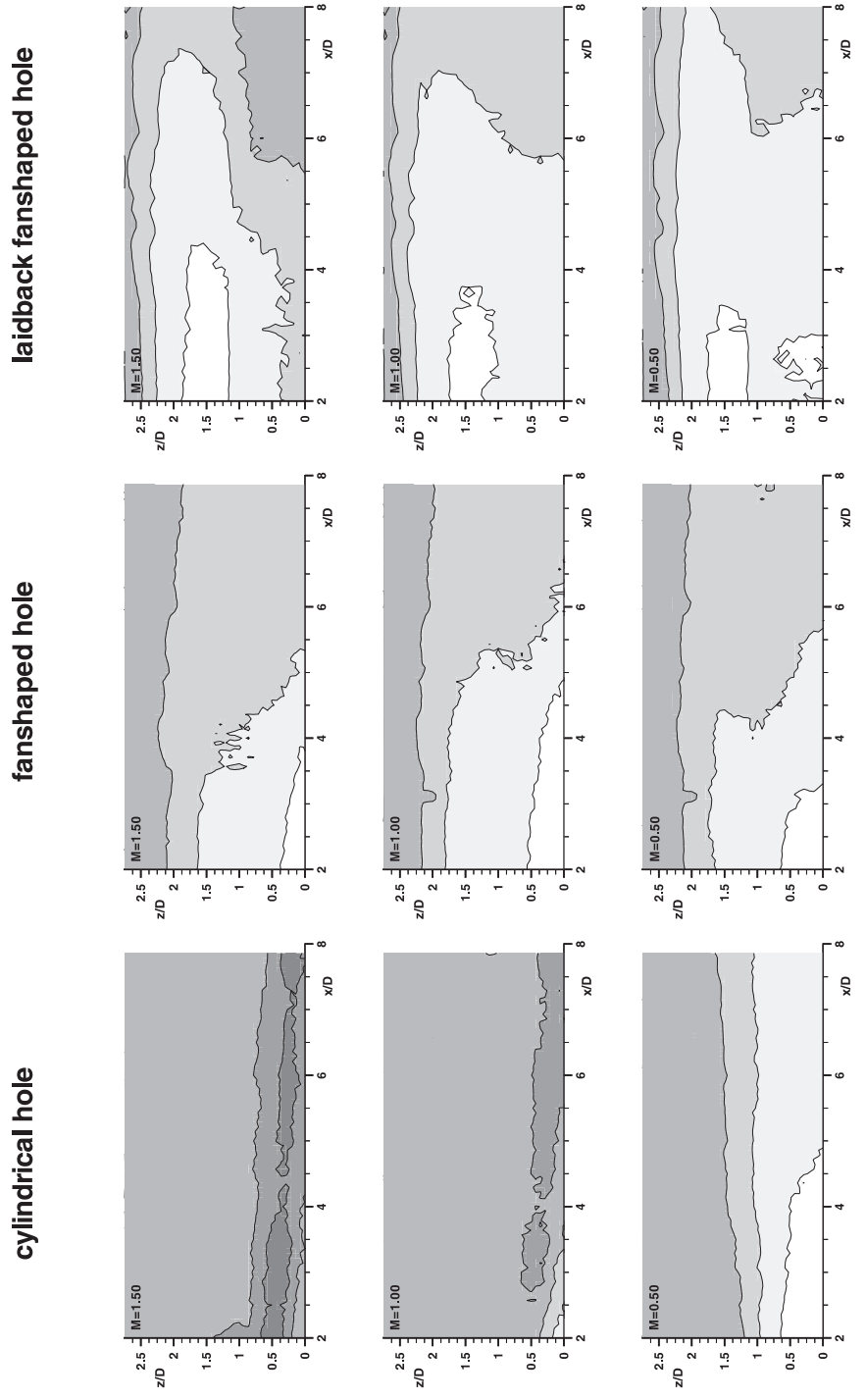

Fig. 4. Local heat transfer coefficients h_f/h_0 for the cylindrical, fanshaped, and laidback fanshaped hole at $Ma_m = 0.6$, $Ma_c = 0.0$.

Table 2

	α (deg)	s/D	DR	Ma_m
Present study	30	–	1.85	0.6
Ekkad et al. (1997b)	35	4	0.98, 1.46	<0.1
Hay et al. (1985)	35	3	1.0	<0.1
Eriksen and Goldstein (1974)	35	3	1.0	<0.2
Ammari et al. (1990)	35	3	1.52	<0.1
Goldstein and Taylor (1982)	35	3	1.0	<0.1

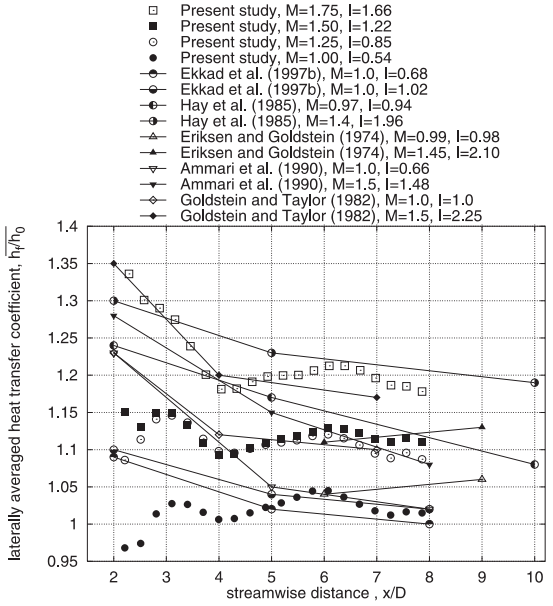

Fig. 5. Comparison of laterally averaged heat transfer coefficients $\overline{h_f/h_0}$ of the cylindrical hole to published data.

supply. The results confirm that the way the coolant is supplied to the hole affects the behavior of the ejected jet as pointed out in an earlier study (Gritsch et al., 1998).

4.4. Spatially averaged heat transfer coefficients

Spatially averaged heat transfer coefficients are calculated by averaging local heat transfer coefficients over the surface downstream of the injection location ($x/D = 2 \ldots 8$, $z/D = \pm 2.75$).

$$\frac{\overline{\overline{h_f}}}{h_0} = \frac{1}{6}\int_{x/D=2}^{x/D=8} \frac{\overline{h_f}}{h_0}(x/d)\,\mathrm{d}(x/D). \tag{9}$$

These values $\overline{\overline{h_f/h_0}}$ are plotted versus blowing ratio in Fig. 9. The slope of the curves is similar to those in Fig. 7. The benefits of both shaped holes as compared to the cylindrical hole become obvious at high blowing ratios. The heat transfer to the surface downstream of the shaped holes is only 75% of the cylindrical hole. The slope of the curves for both shaped holes is about the same, the level for the laidback fanshaped hole, however, is lower, particularly at low blowing ratios.

4.5. Overall film-cooling performance

To evaluate the overall performance of the film-cooling hole geometries studied, present results from the heat transfer coefficient measurements as well as results of film-cooling effectiveness measurements taken from Gritsch et al. (1998) are used to calculate $h/h_0 = f(\Theta)$ and subsequently NHFR =

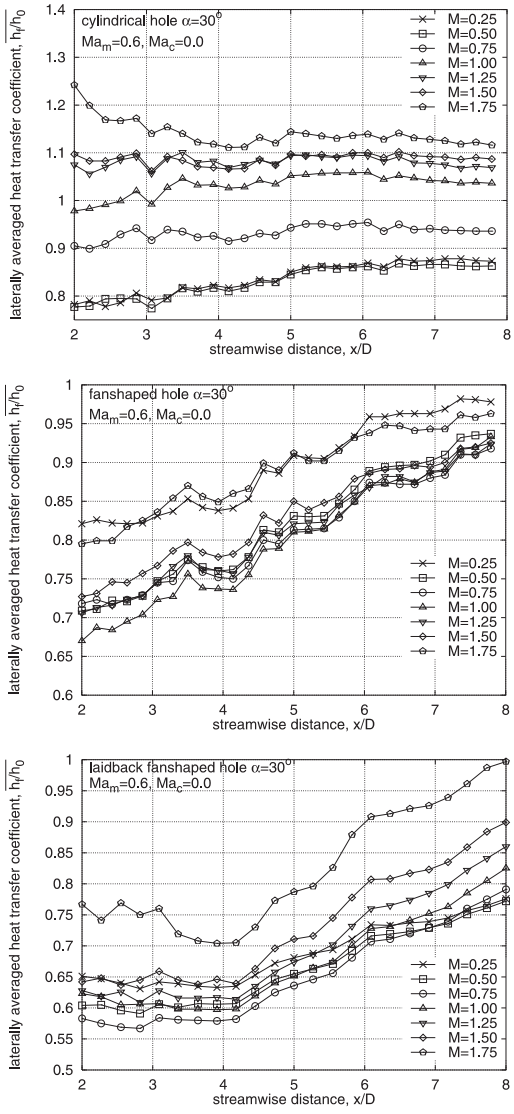

Fig. 6. Laterally averaged heat transfer coefficients $\overline{h_f/h_0}$ for the cylindrical, fanshaped and laidback fanshaped hole at $Ma_m = 0.6$, $Ma_c = 0.0$.

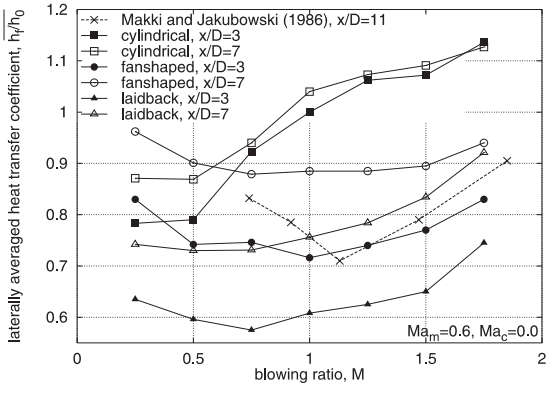

Fig. 7. Effect of blowing ratio M on laterally averaged heat transfer coefficient $\overline{h_f/h_0}$ for the three holes at $Ma_m = 0.6$, $Ma_c = 0.0$.

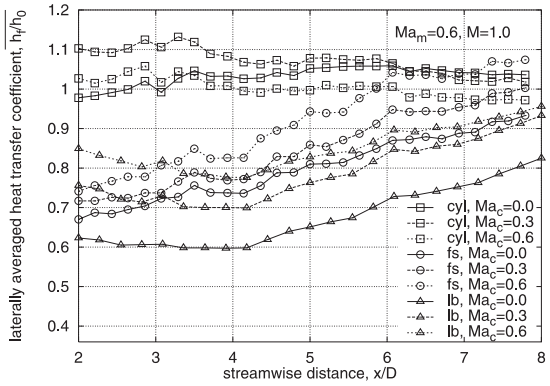

Fig. 8. Effect of coolant supply passage Mach number Ma_c on laterally averaged heat transfer coefficient $\overline{h_f/h_0}$ for the three holes at $Ma_m = 0.6$, $M = 1.0$.

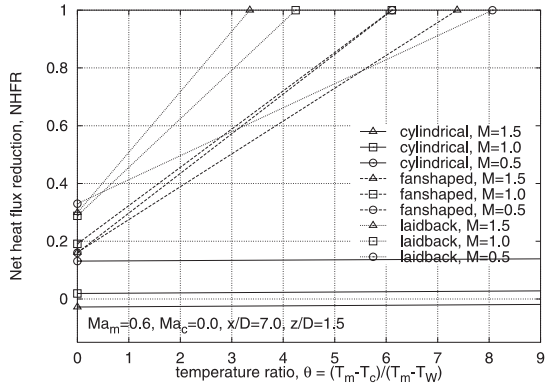

Fig. 11. Variation of NHFR with Θ for the three holes studied at $x/D = 7.0$, $z/D = 1.5$, $Ma_m = 0.6$, $Ma_c = 0.0$.

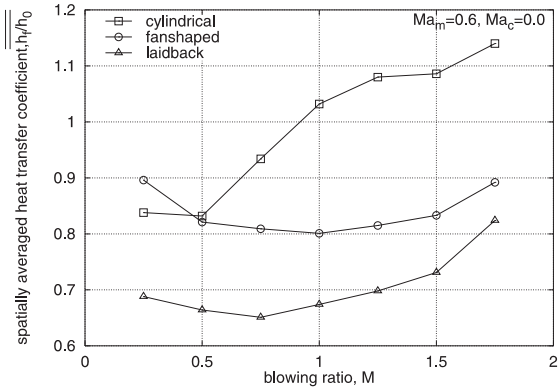

Fig. 9. Effect of blowing ratio M on spatially averaged heat transfer coefficient $\overline{h_f/h_0}$ for the three holes at $Ma_m = 0.6$, $Ma_c = 0.0$.

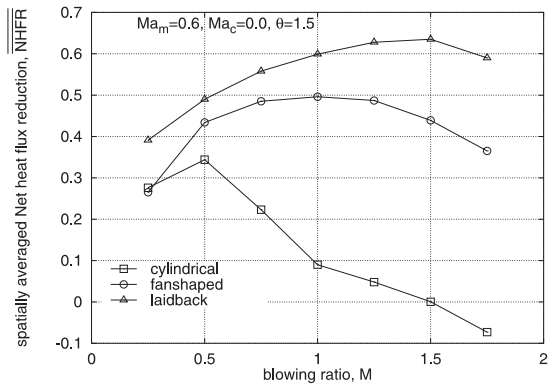

Fig. 12. Effect of blowing ratio M on spatially averaged $\overline{\overline{NHFR}}$ for the three holes at $\Theta = 1.5$, $Ma_m = 0.6$, $Ma_c = 0.0$.

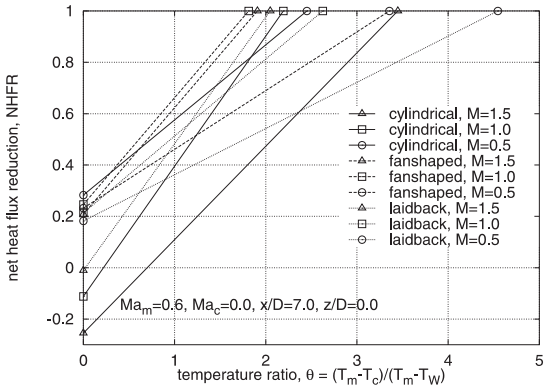

Fig. 10. Variation of NHFR with Θ for the three holes studied at $x/D = 7.0$, $z/D = 0.0$, $Ma_m = 0.6$, $Ma_c = 0.0$.

$f(\Theta)$. A centerline position $(z/D = 0)$ at $x/D = 7$ is chosen to compare the different hole geometries (Fig. 10). When looking at the range of practical relevance, i.e. $\Theta = 1 \ldots 2$, the performance of the fanshaped hole at medium to high blowing ratios is best (low h/h_0 and high NHFR). But also the cylindrical hole at low to medium blowing ratios and the laidback fanshaped hole at medium to high blowing ratios provide reasonable protection of the surface. The cylindrical hole at high blowing ratios as well as fanshaped and laidback fanshaped holes at low blowing ratios, however, show only poor performance.

The improved off-centerline performance of the laidback fanshaped hole as compared to the fanshaped hole becomes obvious when NHFR is plotted versus Θ (Fig. 11) at an off-centerline position $(x/D = 7,\ z/D = 1.5)$. This is due to the improved lateral spreading of the jet exiting the hole as compared to the fanshaped hole. At this location, very small NHFR values are found for the cylindrical hole in the relevant Θ range. For the highest blowing ratio $(M = 1.5)$, negative NHFR values indicate an ineffective use of coolant, since the injected jet is not able to reduce the surface temperature significantly but, on the other hand, augments the heat transfer to the surface.

A spatially averaged net heat flux reduction

$$\overline{\overline{NHFR}} = 1 - \frac{\overline{\overline{h_f}}}{h_0}\left(1 - \overline{\overline{\eta}}\Theta\right) \tag{10}$$

is defined by using the spatially averaged heat transfer coefficient $\overline{\overline{h_f/h_0}}$ and the spatially averaged film-cooling effectiveness $\overline{\overline{\eta}}$ calculated from the data of Gritsch et al. (1998). Setting Θ to a typical value of 1.5 for gas turbine blade applications the key findings of the present investigation are summarized in Fig. 12, which shows the effect of blowing ratio on the overall performance of the three holes. The superiority of both shaped holes at medium to high blowing ratios due to the very poor overall

film-cooling performance of the cylindrical hole is clearly demonstrated. Optimum performance for the shaped holes is achieved at blowing ratios of $M = 1.0$ (fanshaped hole) and $M = 1.5$ (laidback fanshaped hole). As mentioned before, the improved lateral spreading of the jet ejected through the laidback hole causes an increased net heat flux reduction as compared to the fanshaped hole, particularly at high blowing ratios.

5. Conclusions

The present experimental study was conducted to investigate three film-cooling hole geometries including a cylindrical hole and two holes with a diffuser shaped exit portion in terms of local heat transfer coefficients as well as overall cooling performance in the vicinity of the injection location. Tests were performed at an engine like coolant-to-mainflow temperature ratio of 0.54 (DR = 1.85) over a range of blowing ratios of $M = 0.25 \ldots 1.75$. Additionally, the effect of internal coolant supply channel Mach number was investigated. The results revealed that

- holes with expanded exits have profoundly lower heat transfer coefficients at elevated blowing ratios as compared to a cylindrical hole;
- the laidback fanshaped hole provides better lateral spreading of the jet as compared to the fanshaped hole and, therefore, lower laterally averaged heat transfer coefficients;
- combining the effects of reduced heat transfer coefficients and increased film-cooling effectiveness, holes with expanded exits provide significantly improved overall film-cooling performance at elevated blowing ratios as compared to a cylindrical hole;
- coolant crossflow Mach number has an impact on film-cooling performance in the near-hole region, particularly for the shaped holes. Therefore, crossflow at the hole entry side has to be taken into account when modeling film-cooling at engine representative conditions.

Acknowledgements

This study was partly funded by the European Union through grant by the Brite Euram program "Investigation of the Aerodynamics and Cooling of Advanced Engine Turbine Components" under Contract AER2-CT92-0044.

References

Ammari, H.D., Hay, N., Lampard, D., 1990. The effect of density ratio on the heat transfer coefficient from a film-cooled flat plate. ASME Journal of Turbomachinery 112, 444–450.

Burd, S.W., Simon, T.W., 1997. The Influence of coolant supply geometry on film coolant exit flow and surface adiabatic effectiveness. ASME Paper 97-GT-25.

Cho, H.H., Goldstein, R.J., 1995. Heat (mass) transfer and film cooling effectiveness with injection through discrete holes: Part II – On the exposed surface. ASME Journal of Turbomachinery 117, 451–460.

Choe, H., Kays, W.M., Moffat, R.J., 1974. The superposition approach to film-cooling. ASME Paper 74-WA/GT-27.

Eckert, E.R.G., 1984. Analysis of film cooling and full-coverage film cooling of gas turbine blades. ASME Journal of Engineering for Gas Turbines and Power 106, 206–213.

Ekkad, S.V., Zapata, D., Han, J.C., 1997a. Film effectiveness over a flat surface with air and CO_2 injection through compound angle holes using a transient liquid crystal image method. ASME Journal of Turbomachinery 119, 587–593.

Ekkad, S.V., Zapata, D., Han, J.C., 1997b. Heat transfer coefficients over a flat surface with air and CO_2 injection through compound angle holes using a transient liquid crystal image method. ASME Journal of Turbomachinery 119, 580–586.

Eriksen, V.L., Goldstein, R.J., 1974. Heat transfer and film cooling following injection through inclined circular tubes. ASME Journal of Heat Transfer 96, 239–245.

Forth, C.J.P., Loftus, P.J., Jones T.V., 1985. The effect of density ratio on the film-cooling of a flat plate. Heat Transfer and Cooling in Gas Turbines AGARD-CP-390 Paper 10.

Giebert, D., Gritsch, M., Schulz, A., Wittig, S., 1997. Film-cooling from holes with expanded exits: comparison of computational results with experiment. ASME Paper 97-GT-163.

Goldstein, R.J., 1971. Film cooling. Advances in Heat Transfer 7, 321–379.

Goldstein, R.J., Eckert, E.R.G., Burggraf, F., 1974. Effects of hole geometry and density on three-dimensional film cooling. International Journal of Heat Mass Transfer 17, 595–607.

Goldstein, R.J., Taylor, J.R., 1982. Mass transfer in the neighborhood of jets entering a crossflow. ASME Journal of Heat Transfer 104, 715–721.

Gritsch, M., Baldauf, S., Martiny, M., Schulz, A., Wittig, S., 1999. The superposition approach to local heat transfer coefficients in high density ratio film-cooling flows, ASME Paper 99-GT-168.

Gritsch, M., Schulz, A., Wittig, S., 1998. Adiabatic wall effectiveness measurements of film-cooling holes with expanded exits. ASME Journal of Turbomachinery 120, 549–556.

Haller, B.R., Camus, J.J., 1983. Aerodynamic loss penalty produced by film cooling transonic turbine blades. ASME Paper 83-GT-77.

Häring, M., Bölcs, A., Harasgama, S.P., Richter, J., 1995. Heat transfer measurements on turbine airfoils using the naphtalene sublimation technique. ASME Journal of Turbomachinery 117, 432–439.

Hay, N., Lampard, D., 1995. The discharge coefficient of flared film cooling holes. ASME Paper 95-GT-15.

Hay, N., Lampard, D., Benmansour, S., 1983. Effect of crossflows on the discharge coefficient of film cooling holes. ASME Journal of Engineering for Power 105, 243–248.

Hay, N., Lampard, D., Macleod, N., 1993. The swollen polymer technique and its use for heat transfer investigations on film cooled surfaces. Heat Transfer and Cooling in Gas Turbines, AGARD-CP-527 Paper 19.

Hay, N., Lampard, D., Saluja, C.L., 1985. Effects of cooling films on the heat transfer coefficient on a flat plate with zero mainstream pressure gradient. Journal of Engineering for Gas Turbines and Power 107, 104–110.

Hyams, D.G., Leylek, J.H., 1997. A detailed analysis of film cooling physics Part III: Streamwise injection with shaped holes. ASME Paper 97-GT-271.

Kays, W.M., Crawford, M.E., 1980. Convective Heat and Mass Transfer. McGraw-Hill, New York.

Kline, S.J., McClintock, F.A., 1953. Describing uncertainties in single-sample experiments. Mechanical Engineering 75, 3–8.

Kohli, A., Thole, K.A., 1997. A CFD investigation on the effects of entrance crossflow directions to film-cooling holes. In: Proceedings of the 32nd National Heat Transfer Conference. Baltimore, MD, 10–12 August 1997.

Liess, C., 1975. Experimental investigation of film cooling with ejection from a row of holes for the application to gas turbine blades. ASME Journal of Engineering for Power 97, 21–27.

Ligrani, P.M., Subramanian, C.S., Craig, D.W., Kaisuwan, P., 1991. Effects of vortices with different circulations on heat transfer and injectant downstream of a single film-cooling hole in a turbulent boundary layer. ASME Journal of Heat Transfer 113, 79–90.

Makki, Y.H., Jakubowski, G., 1986. An experimental study of film cooling from diffused trapezoidal shaped holes. AIAA Paper 86-1326.

Martiny, M., Schiele, R., Gritsch, M., Schulz, A., Wittig, S., 1996. In situ calibration for quantitative infrared thermography. QIRT'96 Eurotherm Seminar No. 50 Stuttgart, Germany, 2–5 September 1996.

Martiny, M., Schulz, A., Wittig, S., Dilzer, M., 1997. Influence of a mixing-jet on film cooling. ASME Paper 97-GT-247.

Metzger, D.E., Fletcher, D.D., 1971. Evaluation of heat transfer for film-cooled turbine components. Journal of Aircraft 8, 33–38.

Scherer, V., Wittig, S., Morad, K., Mikhael, N., 1991. Jets in a crossflow: effects of hole spacing to diameter ratio on the spatial distribution of heat transfer. ASME Paper 91-GT-356.

Schmidt, D.L., Sen, B., Bogard, D.G., 1996. Film cooling with compound angle holes: adiabatic effectiveness. ASME Journal of Turbomachinery 118, 807–813.

Sen, B., Schmidt, D.L., Bogard, D.G., 1996. Film cooling with compound angle holes: heat transfer. ASME Journal of Turbomachinery 118, 800–806.

Shen, J.R., Ireland, P.T., Wang, Z., Jones, T.V., 1991. Heat transfer coefficient enhancement in a gas turbine blade cooling passage due to film cooling holes. In: Turbomachinery: Latest Developments in a Changing Scene, Paper C 423/040, Proceedings of the Institution of Mechanical Engineers.

Teekaram, A.J.H., Forth, C.J.P., Jones, T.V., 1989. The use of foreign gas to simulate the effects of density ratios in film cooling. ASME Journal of Turbomachinery 111, 57–61.

Thole, K.A., Gritsch, M., Schulz, A., Wittig, S., 1997. Effect of a crossflow at the entrance to a film-cooling hole. ASME Journal of Fluids Engineering 119, 533–541.

Thole, K.A., Gritsch, M., Schulz, A., Wittig, S., 1998. Flowfield measurements for film-cooling holes with expanded exits. ASME Journal of Turbomachinery 120, 327–336.

Wittig, S., Schulz, A., Gritsch, M., Thole, K.A., 1996. Transonic film-cooling investigations: effects of hole shapes and orientations. ASME Paper 96-GT-222.